

EMPIRICAL VERIFICATION OF THE Fe II OSCILLATOR STRENGTHS IN THE *FUSE* BANDPASS¹

J. CHRISTOPHER HOWK, KENNETH R. SEMBACH, KATHERINE C. ROTH, AND JEFFREY W. KRUK

Department of Physics and Astronomy, The Johns Hopkins University, 3400 North Charles Street, Baltimore, MD 21218;
 howk@pha.jhu.edu, sembach@pha.jhu.edu, kroth@pha.jhu.edu, kruk@pha.jhu.edu

Received 2000 June 16; accepted 2000 July 18

ABSTRACT

We report empirical determinations of atomic oscillator strengths, or f -values, for 11 ground-state transitions of Fe II in the wavelength range $1050 \lesssim \lambda \lesssim 1150$ Å. We use ultraviolet absorption-line observations of interstellar material toward stars in the Galaxy and the Magellanic Clouds taken with *Copernicus*, the Goddard High Resolution Spectrograph on board the *Hubble Space Telescope*, and the *Far-Ultraviolet Spectroscopic Explorer*. We derive absolute oscillator strengths by a combination of the apparent optical depth, component-fitting, and curve-of-growth fitting techniques. Our derived oscillator strengths are generally in excellent agreement with recent theoretical calculations by Raassen & Uylings using the orthogonal operator technique. However, we identify three of the 11 transitions studied here whose f -values seem to be incompatible with these calculations by as much as a factor of 2. We suggest revisions to these f -values based on our analysis.

Subject headings: atomic data — ISM: abundances — ISM: atoms — ultraviolet: ISM

1. INTRODUCTION

The measurement and analysis of absorption lines provides the basis for much of our understanding of the content, physical conditions, and evolution of the gas-phase interstellar medium (ISM) in galaxies. Measurements of gas-phase abundances using such techniques have allowed us to study the fundamental “cosmic” abundances of the solar neighborhood (e.g., Meyer, Cardelli, & Sofia 1997; Meyer, Jura, & Cardelli 1998) and the composition and processing of interstellar dust in the warm neutral medium (e.g., Sofia, Cardelli, & Savage 1994; Sembach & Savage 1996; Fitzpatrick 1997; Howk, Savage, & Fabian 1999) and the warm ionized medium (Howk & Savage 1999). Using absorption-line measurements from the *International Ultraviolet Explorer* and the *Hubble Space Telescope* (HST), quality abundance measurements have been extended in a few cases to the ISM of the Magellanic Clouds (Roth & Blades 1995; Welty et al. 1999a) and to the high-velocity cloud system of the Galaxy (Lu et al. 1998; Wakker et al. 1999). The latter examples are potentially important as low-redshift comparisons for the abundances derived in the damped Ly α systems (e.g., Lu et al. 1996; Pettini et al. 1997, 1999; Prochaska & Wolfe 1999), which can be used to study the chemical evolutionary history of the universe over most of a Hubble time.

The recently launched *Far-Ultraviolet Spectroscopic Explorer* (*FUSE*; see Moos et al. 2000; Sahnou et al. 2000), a dedicated spectroscopic observatory operating in the wavelength range 905–1187 Å, will provide a wealth of data on gas-phase abundances of abundant elements in the local universe. Of these, iron is particularly important since it is both an indicator of the overall metal enrichment of the gas as well as a significant constituent of interstellar dust grains (Savage & Sembach 1996). *FUSE* will observe interstellar clouds toward more than 50 stars in the Magellanic Clouds (e.g., Friedman et al. 2000) and tens of objects projected

against high-velocity clouds (e.g., Murphy et al. 2000; Sembach et al. 2000). *FUSE* will also provide measurements of the abundances in low-redshift intergalactic absorbers (e.g., Oegerle et al. 2000; Shull et al. 2000). *FUSE* has sufficient resolution ($\lambda/\Delta\lambda \gtrsim 15,000$) to give reliable ionic column densities in many cases, if the adopted oscillator strengths are reliable.

While most of the near-ultraviolet (NUV; $\lambda \gtrsim 1200$ Å) ground-state transitions of Fe II used to determine interstellar abundances have well-determined f -values that are tied to absolute laboratory measurements (Bergeson, Mullman, & Lawler 1994; Bergeson et al. 1996; Mullman, Sakai, & Lawler 1997), the far-ultraviolet (FUV; $\lambda \lesssim 1200$ Å) transitions of Fe II are not as well constrained. In his new compilation of atomic oscillator strengths for use in absorption-line measurements, D. Morton (2000, in preparation) adopts the theoretical calculations of Raassen & Uylings (1998, hereafter RU98) in this wavelength range. These calculations, performed using the orthogonal operator technique with experimentally determined energy levels, provide results that agree well with the laboratory measurement of many of the NUV transitions of both Fe II and Co II (with average deviations of 10% or less; see RU98).

Even though the agreement between theory and laboratory measurements for the NUV lines is encouraging, an experimental check on the f -values of the commonly observed Fe II transitions in the *FUSE* bandpass is desirable. In this work we have empirically determined the absolute f -values of several FUV ground-state transitions of Fe II. Our emphasis is on those transitions in the wavelength range $1100 \lesssim \lambda \lesssim 1150$ Å, which contains transitions spanning more than a factor of 30 in oscillator strength, though we also present results for a few shorter wavelength transitions. Table 1 summarizes the results of this study, giving our final derived f -values and comparing our values with empirical and theoretical values from the literature. In general, we find very good agreement between our empirically derived oscillator strengths and the theoretical results of RU98. There are several exceptions, including the transitions at 1112.048, 1121.975, and 1127.098 Å.

¹ Based on observations made with the NASA/ESA *Hubble Space Telescope*, obtained from the data archive at the Space Telescope Science Institute. STScI is operated by the Association of Universities for Research in Astronomy, Inc. under the NASA contract NAS 5-26555.

TABLE 1
RECOMMENDED Fe II OSCILLATOR STRENGTHS FOR THE *FUSE* BANDPASS

					LITERATURE f_{λ} -VALUES ^f					
λ_c ^a	UPPER TERM ^b	NUMBER ^c	INSTRUMENT ^d	f_{λ} ^e	RU98	Kurucz	Lugger et al.	van Buren	Shull et al.	
1055.262	$3d^5 4s4p$	$^6P^o_{7/2}$	2	C	0.0075(14)	0.00615	0.0108	0.0074(10)	0.0092(9)	0.0080(12)
1063.972	$3d^5 4s4p$	$^6D^o_{7/2}$	1	C	0.0037(18)	0.00475	0.00373	...	0.0041(6)	0.0045(9)
1096.877	$3d^6 5p$	$^6P^o_{7/2}$	3	C	0.032(4)	0.0327	0.0565	0.032(5)	0.0370(15)	0.032(5)
1112.048	$3d^6 5p$	$^6F^o_{11/2}$	12	F	0.0062(9)	0.00446	0.00826
1121.975	$3d^5 4s4p$	$^6P^o_{7/2}$	17	CGF	0.0202(20)	0.0290	0.0189	0.0203(12)	0.0227(16)	0.020(3)
1125.448	$3d^6 5p$	$^6D^o_{7/2}$	2	CG	0.016(3)	0.0156	0.0261	...	0.0205(16)	0.011(3)
1127.098	$3d^6 5p$	$^6D^o_{9/2}$	12	CGF	0.0028(3)	0.00112	0.00228
1133.665	$3d^5 4s4p$	$^6D^o_{7/2}$	3	CG	0.0055(8)	0.0047	0.0125	0.0048(5)	0.0074(11)	0.0060(9)
1142.366 ^g	$3d^5 4s4p$	$y^6 F^o_{7/2}$	18	CGF	0.0042(3)	0.00401	0.00573	0.0050(5)	0.0060(7)	0.0050(15) ^h
1143.226	$3d^5 4s4p$	$y^6 F^o_{9/2}$	5	CG	0.0177(12)	0.0192	0.0268	0.0133(7)	0.0200(18)	0.013(4)
1144.938	$3d^5 4s4p$	$y^6 F^o_{11/2}$	5	G	0.106(10)	0.1090	0.1122	0.1050(5)	0.126(9)	0.105(21)

^a Vacuum wavelengths (in Å) from D. Morton 2000, in preparation.

^b Designation of the upper term of the transition. All transitions arise from the ground state, $3d^6(a^5D)4s^6D_{9/2}$.

^c Number of individual f_λ^i determinations used in deriving the final value presented in this table.

^d The instrument(s) used in deriving each f_λ , where C, G, and F denote *Copernicus*, GHRS, and *FUSE*, respectively.

^e Final derived oscillator strengths from the current work. The numbers in parentheses denote the uncertainties in the last digit(s).

^f Selected literature values of Fe II oscillator strengths for comparison with those derived in the current work. The columns give literature f -values from the calculations of Raassen & Uylings 1998 (adopted by Morton 2000) and Kurucz 1988, and from the empirical (astrophysical) determinations by Lugger et al. 1982, van Buren 1986, and Shull et al. 1983, respectively. The numbers in parentheses denote the uncertainties in the last digit(s).

^g Cardelli & Savage 1995 have also used the GHRS to empirically estimate this f -value. They derive $f_{\lambda 1142} = 0.00247(32)$ based only on the sight line toward β^1 Scorpii using a curve-of-growth fit.

^h Shull et al. 1983 give a value of 0.050(15) in their Table 3. This is a typographical error that has been corrected for the current table (J. M. Shull 2000, private communication).

We have used a multistep approach to derive the oscillator strengths given in Table 1. First, we used observations of three nearby stars (ζ Oph, δ Ori, and μ Col) taken with the Goddard High Resolution Spectrograph (GHRS) on board the *HST* and literature measurements from the *Copernicus* satellite to determine the f -values of several FUV transitions using apparent optical depth (AOD; Savage & Sembach 1991), component-fitting (see Howk et al. 1999), and curve-of-growth fitting methods (e.g., see Jenkins 1986). The oscillator-strength measurements were placed on an absolute scale by reference to NUV transitions of Fe II whose oscillator strengths have been measured in the laboratory (Bergeson et al. 1994, 1996; Mullman et al. 1997). This analysis provided reliable f -value determinations for Fe II $\lambda\lambda 1125$, 1133, 1143, and 1144² that are in excellent agreement with the theoretical calculations of RU98. This portion of our study is presented in § 2.

With these well-determined absolute f -values in hand, we then used *FUSE* observations of 15 stars and curve-of-growth fitting methods to place the 1112, 1121, 1127, and 1142 Å transitions on the same absolute oscillator-strength scale. Most of the sight lines used for determining these f -values are toward stars in the Large Magellanic Cloud (LMC; 12 of 15 stars); the remaining stars are located in the Small Magellanic Cloud (SMC; two stars) and in the low halo of the Milky Way (one object). We find an oscillator strength for the 1142 Å transition that agrees with the calculations of RU98, although the other three transitions examined require adjustments of 30%–140%. This phase of the study is presented in § 3. We summarize our work and discuss its implications in § 4.

2. GHRS AND *Copernicus* MEASUREMENTS OF Fe II OSCILLATOR STRENGTHS AT FAR-ULTRAVIOLET WAVELENGTHS

In this section we derive the absolute oscillator strengths of several FUV Fe II transitions using archival GHRS data and literature measurements from the *Copernicus* satellite. For this treatment, we have chosen to focus on three well-observed, well-studied sight lines for which high-quality GHRS data and accurate *Copernicus* measurements exist, covering both the FUV lines with unknown f -values and the NUV lines with measured f -values. The three sight lines used here are the μ Col (Shull & York 1977; Howk et al. 1999), ζ Oph (Morton 1975; Savage, Cardelli, & Sofia 1992), and δ Ori (see Bohlin et al. 1983) sight lines.

Our reduction of the archival GHRS data is discussed in § 2.1. We have used three independent techniques to derive absolute Fe II oscillator strengths with these data. These are the three methods commonly used for deriving ionic column densities and include the apparent optical depth method of Savage & Sembach (1991), which we apply to the determination of f -values using the μ Col data sets in § 2.2, component-fitting techniques, which are applied to the μ Col sight line in § 2.3, and curve-of-growth fitting, which is applied to all three sight lines in § 2.4. We summarize the results of our GHRS and *Copernicus* analysis in § 2.5.

2.1. GHRS Observations and Data Reduction

We have used archival GHRS observations of μ Col (HD 38666), δ Ori (HD 36486), and ζ Oph (HD 149757) to measure equivalent widths of FUV (and some NUV) Fe II transitions along these three sight lines. Although the nominal short-wavelength limit of the GHRS is 1150 Å, given the low efficiency of the MgF₂ coatings of the *HST* optics at wavelengths shortward of 1150 Å, observations at such wavelengths are possible for sufficiently bright targets.

² We will often refer to transitions by rounding the values of D. Morton (2000, in preparation) for their wavelengths downward. Hence, Fe II $\lambda 1144$ refers to the line at 1144.938 Å.

Howk et al. (1999) have demonstrated this capability, presenting GHRs observations of Fe III λ 1122, the λ 1134 triplet of N I, and Fe II λ 1133, 1143, and 1144 toward the low-halo star μ Col.

A log of the GHRs observations used in this work is given in Table 2. For the sight lines toward μ Col and ζ Oph, details of the observations at $\lambda > 1200$ Å are given by Howk et al. (1999) and Savage et al. (1992). The GHRs data toward δ Ori are presented here for the first time.

Our reduction of the archival GHRs data follows that of Howk et al. (1999). The basic calibration makes use of the standard CALHRS routine³ using the best calibration reference files as of the end of the GHRs mission. The CALHRS processing includes conversion of raw counts to count rates and corrections for particle radiation contamination, dark counts, known diode nonuniformities, paired pulse events, and scattered light. The wavelength calibration was derived from the standard calibration tables. The absolute wave-

length scale should be accurate to $\sim \pm 1$ resolution element (see Table 2).

The final data reduction was performed using software developed and tested at the University of Wisconsin–Madison. This includes the merging of individual spectra and allowing for additional refinements to the scattered-light correction for echelle-mode observations. The inter-order scattered-light removal in GHRs echelle-mode data discussed by Cardelli, Ebbets, & Savage (1990, 1993) is based on extensive preflight and in-orbit analysis of GHRs data and is used by the CALHRS routine; the coefficients derived by these authors are appropriate for observations made through the Small Science Aperture (SSA). The scattered-light coefficients for the Large Science Aperture (LSA) observations of μ Col used in this work are given in Table 2 of Howk et al. (1999). The first-order G140M, G160M, and G200M holographic gratings have very little scattered light, and no adjustment has been made to the zero point of spectra taken with these gratings.

In all cases the GHRs absorption-line data were normalized with low-order (< 5) Legendre polynomial fits to the local stellar continuum, as discussed by Sembach & Savage (1992, see their Appendix). Figure 1 shows the continuum-

TABLE 2
GHRs OBSERVATION LOG^a

Spectra Range (Å)	Rootname ^b	Exposure Time (s)	Grating	Resolution ^c (km s ⁻¹)	Aperture ^d	COSTAR? ^e
μ Columbae						
1116–1124.....	Z2X30108T	81.6	G140M	16.0	LSA	Yes
	Z2X30109T	81.6	G140M	16.0	LSA	Yes
1131–1137.....	Z2C0011AP	108.8	Ech-A	3.5	LSA	Yes
1142–1148.....	Z2AF011AT	108.8	Ech-A	3.5	LSA	Yes
	Z2C0030RT	108.8	Ech-A	3.5	LSA	Yes
	Z308010OT	108.8	Ech-A	3.5	LSA	Yes
	Z3JN010OT	108.8	Ech-A	3.5	LSA	Yes
δ Orionis A						
1127–1164.....	Z1850107T	217.6	G160M	21.0	SSA	No
2256–2265.....	Z185020KT	13.6	Ech-B	3.5	SSA	No
	Z185020LT	13.6	Ech-B	3.5	SSA	No
	Z185020MT	13.6	Ech-B	3.5	SSA	No
2367–2377.....	Z185020NT	13.6	Ech-B	3.5	SSA	No
	Z185020OT	13.6	Ech-B	3.5	SSA	No
	Z185020PT	13.6	Ech-B	3.5	SSA	No
2599–2609.....	Z185020QT	13.6	Ech-B	3.5	SSA	No
	Z185020RT	13.6	Ech-B	3.5	SSA	No
	Z185020ST	13.6	Ech-B	3.5	SSA	No
ζ Ophiuchi						
1126–1154.....	Z0HU020WM	68.0	G140M	15.0	SSA	No
	Z0HU520UT	68.0	G140M	15.0	SSA	No
1603–1638.....	Z0HU012AT	13.6	G160M	14.0	LSA	No
2241–2279.....	Z0HU013JM	13.6	G200M	11.0	LSA	No
2334–2347.....	Z0XZ010BT	5.6	Ech-B	3.5	SSA	No

^a This table describes the GHRs exposures used in this work. For μ Col and ζ Oph, we list only those data sets covering $\lambda < 1200$ Å. The longer wavelength GHRs data for μ Col are described by Howk et al. 1999, and the ζ Oph data are discussed by Savage et al. 1992.

^b STScI archival rootname.

^c Approximate velocity resolution (FWHM) in km s⁻¹.

^d The entrance aperture used for the observation. Here SSA refers to the Small Science Aperture (pre-COSTAR: 0".24 \times 0".24; post-COSTAR: 0".22 \times 0".22), and LSA refers to the Large Science Aperture (pre-COSTAR: 2".00 \times 2".00; post-COSTAR: 1".74 \times 1".74)

^e Denotes observations taken before (No) or after (Yes) the installation of the Corrective Optics Space Telescope Axial Replacement (COSTAR) unit.

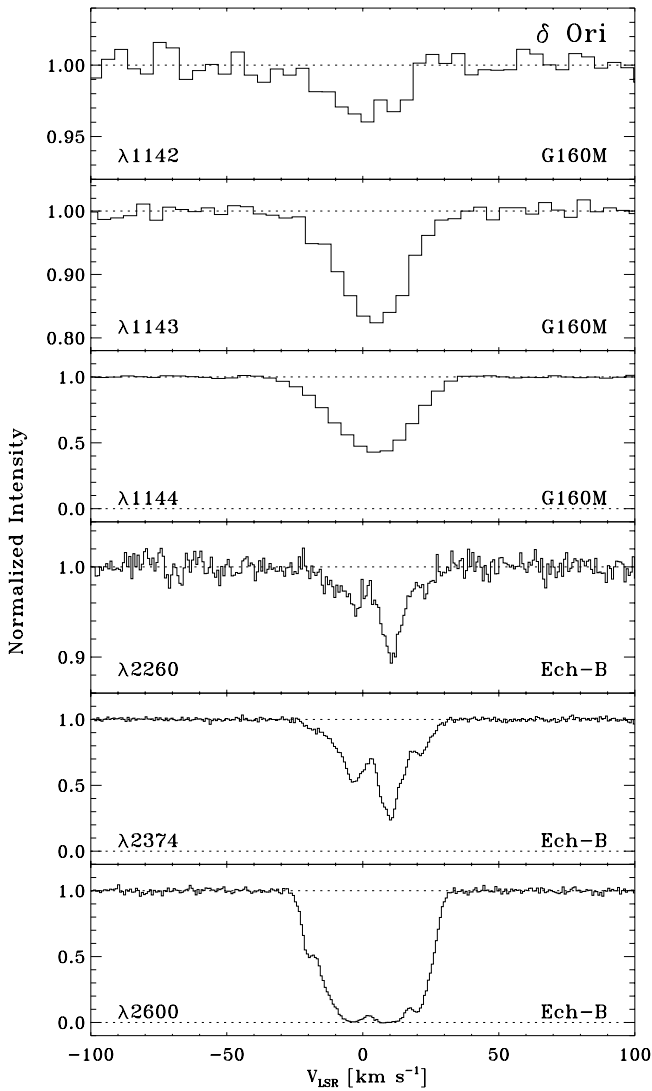


FIG. 1.—Continuum-normalized GHRs absorption-line spectra of the measured Fe II transitions toward δ Ori. The velocity scale is with respect to the local standard of rest (LSR), and no adjustments have been made to the default wavelength calibrations of the data. The Ech-B data have a resolution of $\Delta v \sim 3.5 \text{ km s}^{-1}$; the G160M data have a resolution $\Delta v \sim 21 \text{ km s}^{-1}$.

normalized absorption profiles of the Fe II absorption lines toward δ Ori. The top three profiles, observed with the first-order G160M grating, have a velocity resolution of $\Delta v \sim 21 \text{ km s}^{-1}$, while the lower three lines were observed with the Ech-B echelle grating at a resolution of $\Delta v \sim 3.5 \text{ km s}^{-1}$.

We have measured the equivalent widths for interstellar Fe II absorption lines along these three sight lines following Sembach & Savage (1992); these are given in Table 3. The error estimates include continuum placement uncertainties and the effects of a 2% zero-level uncertainty. Also given are *Copernicus* and GHRs literature measurements for several transitions.

The NUV ($\lambda > 1200 \text{ \AA}$) lines listed in Table 3 are considered reference transitions in our analysis. For these lines, we adopt oscillator strengths derived from the quality laboratory measurements of Mullman et al. (1997) and Bergeson et al. (1994, 1996). The laboratory determinations of

the f -values for these transitions are given in Table 4 along with the f -values calculated by RU98 for comparison.

2.2. Apparent Optical Depth Analysis

The apparent optical depth method for interpreting absorption-line spectra has been discussed by Savage & Sembach (1991) and Jenkins (1996). Its application to empirically deriving atomic oscillator strengths from astrophysical data has been discussed by Cardelli & Savage (1995) and Sofia, Fabian, & Howk (2000). The apparent optical depth, $\tau_a(v)$, an instrumentally blurred version of the true optical depth of an absorption line, is given by

$$\tau_a(v) = -\ln[I(v)/I_0(v)], \quad (1)$$

where $I_0(v)$ is the estimated continuum intensity and $I(v)$ is the observed intensity of the line as a function of velocity. This is related to the apparent column density per unit velocity, $N_a(v)$ [in units of $\text{atoms cm}^{-2} (\text{km s}^{-1})^{-1}$], by

$$N_a(v) = \frac{m_e c}{\pi e^2} \frac{\tau_a(v)}{f \lambda} = 3.768 \times 10^{14} \frac{\tau_a(v)}{f \lambda(\text{\AA})}, \quad (2)$$

where λ is the wavelength in angstroms and f is the atomic oscillator strength. In the absence of unresolved saturated structure the $N_a(v)$ profile of a line is a valid, instrumentally blurred representation of the true column-density distribution as a function of velocity, $N(v)$. Where unresolved saturated structure is present, the values of the $N_a(v)$ profile are lower limits to the true instrumentally blurred values of $N(v)$.

For regions of absorption that are well resolved, i.e., where $N_a(v)$ represents $N(v)$ well,

$$\tau_a(v) \propto \lambda f N(v). \quad (3)$$

If one compares two absorption lines from the same species, the ratio of their apparent optical depths over this well-resolved region should simply be the ratio of their respective values of λf . Hence, the apparent column-density profiles of multiple Fe II transitions can be used to derive relative oscillator strengths.

The sight line toward μ Col exhibits a blend of warm components centered on $v_{\text{LSR}} \approx 3 \text{ km s}^{-1}$ (component 1 of Howk et al. 1999) stretching from $v_{\text{LSR}} \approx -17$ to 16 km s^{-1} . This blend of components is well resolved with the echelle-mode gratings of the GHRs. Howk et al. (1999) have shown that lines of Fe II as strong as $\lambda 2374.461$ ($f = 0.0313$) and $\lambda 2586.650$ ($f = 0.0691$) exhibit no unresolved saturation over this velocity range (see their Fig. 9). Components 2–4 ($v_{\text{LSR}} \approx 16$ – 47) along this sight line show varying degrees of unresolved saturated structure in the strongest lines.

We have used the $N_a(v)$ profiles of Fe II $\lambda\lambda 1143$ and 1144 derived from GHRs echelle-mode observations of the μ Col sight line to determine the f -values of these transitions by comparison with the $N_a(v)$ profiles of several NUV lines of Fe II. We have limited our use of the $N_a(v)$ profiles for determining f -values to those FUV transitions that were observed with the echelle-mode gratings on the GHRs with high signal-to-noise. This restriction is adopted to avoid problems with unresolved saturated structure. This limits our use of the $N_a(v)$ method of deriving oscillator strengths to the observations of Fe II $\lambda\lambda 1143$ and 1144 toward μ Col.

Using the NUV Fe II $\lambda\lambda 2249.877$, 2374.461 , and 1608.451 profiles as reference transitions, we have calculated the value f_i/f_{ref} that minimizes χ^2 for each pair of unknown

TABLE 3
GHRS/*Copernicus* Fe II EQUIVALENT-WIDTH MEASUREMENTS

λ_c^a (Å)	μ Col ^b		δ Ori ^c		ζ Oph ^d	
	W_λ (mÅ)	Instrument ^e	W_λ (mÅ)	Instrument ^e	W_λ (mÅ)	Instrument ^e
1055.262.....	11.2 ± 2.0	<i>Cop</i>	21(±3)	<i>Cop</i>
1063.972.....	7 ± 3.0	<i>Cop</i>
1096.877.....	53 ± 3.0	<i>Cop</i>	30.0 ± 0.7	<i>Cop</i>	52 (±3)	<i>Cop</i>
1121.975.....	34 ± 4.0	G140M	22.4 ± 1.3	<i>Cop</i>	42 (±3)	<i>Cop</i>
1125.448.....	27 ± 4.0	G140M	39 (±3)	<i>Cop</i>
1127.098.....	10.5 ± 2.1	<i>Cop</i> /G140M
1133.665.....	14.0 ± 2.5	Ech-A	6.1 ± 0.5	<i>Cop</i>	15.5 ± 1.9	<i>Cop</i> /G140M
1142.366.....	4.1 ± 0.7	G160M	17.9 ± 1.9	<i>Cop</i> /G140M
1143.226.....	34.8 ± 1.1	Ech-A	20.2 ± 0.7	G160M	37.9 ± 2.2	<i>Cop</i> /G140M
1144.938.....	112.9 ± 2.1	Ech-A	74.7 ± 0.9	G160M	80.7 ± 1.4	G140M
1608.451.....	144.4 ± 2.4	Ech-A	103 ± 3	G160M
2249.877.....	14.2 ± 0.4	Ech-B	22.5 ± 1.1	Ech-B
2260.780.....	21.9 ± 0.6	Ech-B	12.9 ± 0.7	Ech-B	31 ± 4	G200M
2344.214.....	302 ± 4.0	Ech-B	195 ± 4	Ech-B
2374.461.....	182 ± 3.0	Ech-B	125 ± 3.0	Ech-B	149.2 ± 1.3	Ech-B
2586.650.....	291 ± 4.0	Ech-B
2600.173.....	388 ± 5.0	Ech-B	370 ± 7.0	Ech-B

^a Central wavelengths from D. Morton 2000, in preparation.

^b The *Copernicus* equivalent-width measurements toward μ Col are from Shull & York 1977. The GHRS measurements for $\lambda_c > 1133$ Å are from Howk et al. 1999, while the remaining GHRS G140M measurements are from this work.

^c The δ Ori *Copernicus* measurements are from Bohlin et al. 1983, while the GHRS measurements are from this work.

^d The ζ Oph *Copernicus* measurements are from Morton 1975. The $\lambda\lambda 2249$, 2374 Ech-B GHRS measurements are from Savage et al. 1992. The remaining GHRS measurements are from this work. Where no error measurement was quoted for the *Copernicus* equivalent widths we assumed a 1 σ error of 3 mÅ. Such errors are given in parentheses. Both GHRS and *Copernicus* equivalent-width measurements were available for several transitions. In most of these cases the measurements agreed to within 1 σ of the GHRS measurements. Where two measurements are available, and the *Copernicus* data seem of high quality, we averaged the equivalent widths from these two instruments.

^e The instrument with which the measurements were made. In this case *Cop* refers to measurements made with the *Copernicus* satellite, while GHRS measurements are listed according to the grating used: Ech-A, Ech-B, G140M, G160M, or G200M.

(FUV) and reference (NUV) line profiles. We have used only absorption from component 1 ($v_{\text{LSR}} \approx -17$ to 16 km s⁻¹) to avoid potential unresolved saturated structure. The presence of such a structure in the strong $\lambda 1144$ transition would reveal itself through a divergence of the $N_a(v)$ profiles for highest $\tau_a(v)$ of the strong line compared with a weaker transition. We find no evidence for such saturation in the $\lambda 1144$ profile compared with, e.g., the $\lambda 1608$ profile.

TABLE 4
NEAR-ULTRAVIOLET Fe II OSCILLATOR STRENGTHS

λ_c^a (Å)	f_λ^b	Reference ^c	f_{RU98}^d
1608.451.....	0.058(5)	1	0.054
2249.877.....	0.00182(14)	2	0.00218
2260.780.....	0.00244(19)	2	0.00262
2344.214.....	0.114(2)	2	0.125
2374.461.....	0.0313(14)	2	0.0329
2586.650.....	0.0691(25)	2	0.0709
2600.173.....	0.239(4)	2	0.242

^a Central wavelength from Morton 2000.

^b Adopted experimental oscillator strength.

^c Reference for adopted experimental oscillator strengths: (1) Mullman et al. 1997; (2) Bergeson et al. 1996.

^d Theoretical oscillator strength from Raassen & Uylings 1998 for comparison.

However, the noise in the $\lambda 1144$ profile can cause points with high $\tau_a(v)$ to have artificially high optical depths. To avoid biases associated with low signal-to-noise ratio over a limited velocity range, we have restricted our analysis to data points having $\tau_a \leq 2.5$ in determining the f -values using the $\lambda 1144$ profile.

Table 5 summarizes all of our GHRS f -value determinations, giving the RU98 theoretical f -value, the average of our determinations for each line, the individual f -value measurements, and the star, instrument, and method used in deriving those measurements. The oscillator strengths derived as described above are marked AOD (apparent optical depth) in Table 5 and represent the average value of the f -values derived using each of the three reference transitions. For $\lambda\lambda 1143$ and 1144 we derive $f = 0.0206(8)$ and 0.107(4), respectively, using the apparent optical depth method. The errors include contributions from the uncertainties in the reference oscillator strengths as well as the sources of error discussed by Howk et al. (1999).

The $N_a(v)$ profiles for the FUV Fe II lines $\lambda\lambda 1144$ and 1143 are compared with the reference transitions $\lambda\lambda 1608$ and 2374 in Figure 2 using our final f -values from Table 1. The profiles of the reference lines are plotted using open squares, while the circles show the $\lambda\lambda 1144$ and 1143 profiles. For the lines shown in Figure 2, the agreement between the $N_a(v)$ profiles is excellent across the entire velocity range.

TABLE 5
SUMMARY OF GHRS/*Copernicus* RESULTS

λ_c^a (Å)	f_{RU98}^b	$\langle f_\lambda \rangle^c$	$f_\lambda^i{}^d$	Star	Instrument ^e	Method ^f
1055.262.....	0.00615	0.0075(14)[–]	0.0061(16)	μ Col	<i>Cop</i>	CoG
			0.0088(22)	ζ Oph	<i>Cop</i>	CoG
1063.972.....	0.00475	0.0037(18)[–]	0.0037(18)	μ Col	<i>Cop</i>	CoG
1096.877.....	0.0327	0.032(4)[3]	0.034(7)	μ Col	<i>Cop</i>	CoG
			0.028(6)	δ Ori	<i>Cop</i>	CoG
			0.033(9)	ζ Oph	<i>Cop</i>	CoG
1121.975.....	0.0290	0.019(3)[1]	0.018(4)	μ Col	G140M	CoG
			0.019(4)	δ Ori	<i>Cop</i>	CoG
			0.020(5)	ζ Oph	<i>Cop</i>	CoG
1125.448.....	0.0156	0.016(3)[3]	0.014(4)	μ Col	G140M	CoG
			0.018(4)	ζ Oph	<i>Cop</i>	CoG
1127.098.....	0.00112	0.0034(9)[–]	0.0034(9)	ζ Oph	G140M/ <i>Cop</i>	CoG
1133.665.....	0.0047	0.0055(8)[11]	0.0067(18)	μ Col	Ech-A	CoG
			0.0046(10)	δ Ori	<i>Cop</i>	CoG
			0.0052(12)	ζ Oph	G140M/ <i>Cop</i>	CoG
1142.366.....	0.00401	0.0045(8)[–]	0.0031(8)	δ Ori	G160M	CoG
			0.0060(13)	ζ Oph	G140M/ <i>Cop</i>	CoG
1143.226.....	0.0192	0.0177(12)[18]	0.018(4)	μ Col	Ech-A	CoG
			0.0206(8)	μ Col	Ech-A	AOD
			0.0181(13)	μ Col	Ech-A	CF
			0.016(3)	δ Ori	G160M	CoG
			0.016(3)	ζ Oph	G140M/ <i>Cop</i>	CoG
1144.938.....	0.1090	0.106(10)[11]	0.11(3)	μ Col	Ech-A	CoG
			0.107(4)	μ Col	Ech-A	AOD
			0.120(18)	μ Col	Ech-A	CF
			0.09(3)	δ Ori	G160M	CoG
			0.104(17)	ζ Oph	G140M	CoG

^a Vacuum wavelengths (in Å) from D. Morton 2000, in preparation.

^b Theoretical values of f_λ calculated by Raassen & Uylings 1998. These oscillator strengths are adopted in the new compilation of Morton 2000.

^c Average values of f_λ with 1 σ statistical uncertainties of the last digits in parentheses. The standard deviations of the individual measurements f_λ^i about the mean are given in square brackets.

^d Individual measurements f_λ^i of the oscillator strengths with 1 σ errors in the last digit(s) given in parentheses.

^e Instrument used in deriving the individual oscillator-strength estimates; *Cop* refers to data taken with the *Copernicus* satellite, while Ech-A, G140M, and G160M refer to the gratings used in GHRS observations. The *Copernicus* data for μ Col, ζ Oph, and δ Ori are taken from Shull & York 1977, Morton 1975, and Bohlin et al. 1983, respectively.

^f Method used for deriving the individual f -value measurement. f_λ^i : CoG—curve-of-growth fitting; AOD—apparent optical depth/column-density method; and CF—component fitting.

2.3. Component-Fitting Analysis

The component structure of the neutral ISM along the μ Col sight line has been studied through an analysis of nearly 50 lines of 14 species from dominant ionization states (Howk et al. 1999). We make use of the Howk et al. component structure to determine the f -values of the FUV Fe II lines, following Fitzpatrick (1997) and Sofia et al. (2000). This method of analysis is most reliable when using high-resolution data, since the details of the component structure along a sight line can be hidden at lower resolution. Hence we do not apply this method to the FUV intermediate-resolution GHRS data for any of the sight lines, which precludes use of the δ Ori and ζ Oph sight lines for determining f -values in this way.

We use the component-fitting software originally written by E. Fitzpatrick and described by Spitzer & Fitzpatrick (1993) and Fitzpatrick & Spitzer (1997). This code has been updated to account for the post-COSTAR instrumental line-spread function of GHRS observations made through the LSA (see Appendix A of Howk et al. 1999). A model for the interstellar medium along the sight line was constructed

by assuming a number of “clouds,” or components, along the line of sight. Each component was defined by its column density, central velocity, and Doppler spread parameter (b -value). These three parameters were varied for each component until a minimum χ^2 -value between the model, convolved by the instrumental spread function, and the original data was found. In the case of Fe II, which has many ultraviolet transitions, the component structure was tested simultaneously against all of the available absorption profiles (each of which was given an input f -value).

We have derived oscillator strengths of the FUV $\lambda\lambda 1143$ and 1144 transitions by simultaneously fitting all of the Fe II lines (see Table 3 and Howk et al. 1999) observed with the echelle-mode observations, allowing not only the parameters of the component model to vary, but also the f -values of the FUV transitions. The final derived component structure is indistinguishable from the results presented in Tables 5 and 6 of Howk et al. (1999), which is expected given that the same NUV transitions are used here to define the component structure while allowing the FUV f -values to vary in the fit. Table 5 gives the resulting f -values for $\lambda\lambda 1143$ and

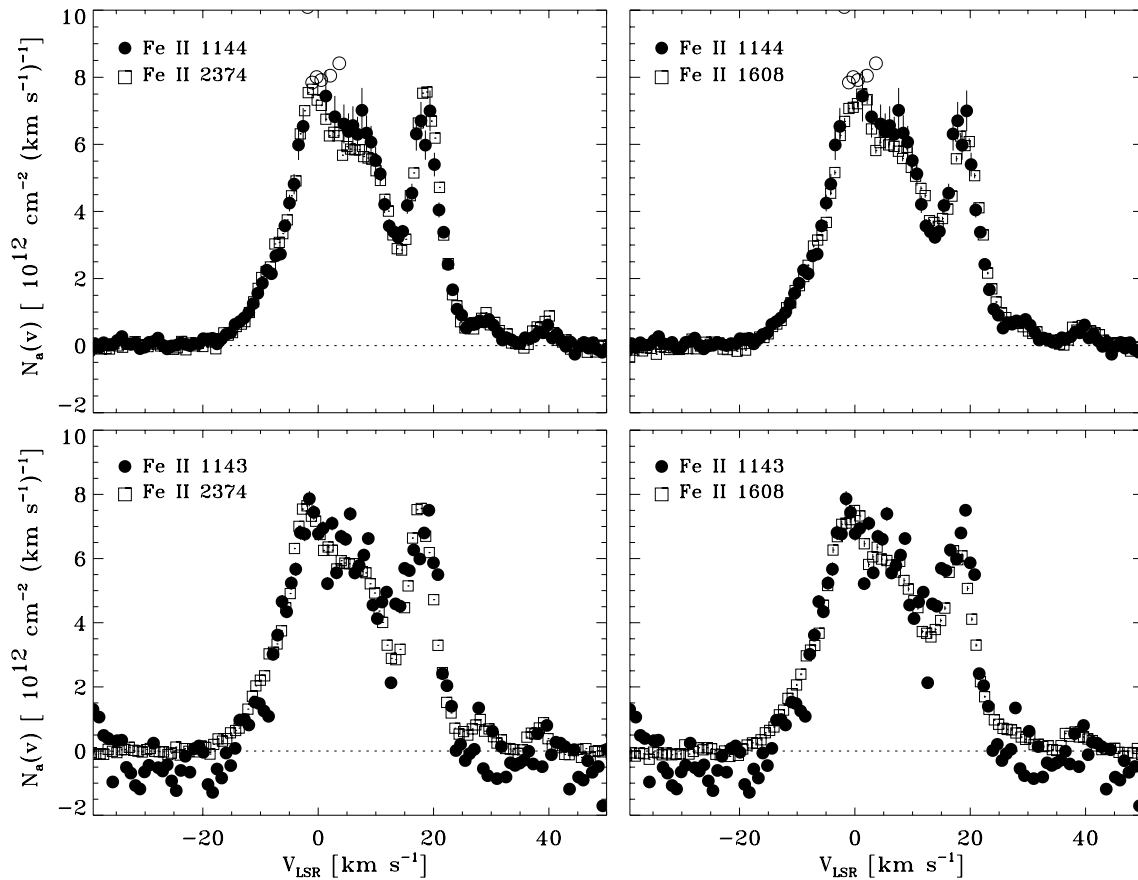


FIG. 2.—Apparent column-density profiles for the FUV transitions of Fe II at 1143.226 and 1144.938 Å compared with the reference lines at 1608.451 and 2374.461 Å for the sight line to μ Col. The circles show the FUV profiles while the open squares denote the reference lines. The open circles in the plots containing the λ 1144 profile show points that were not used in determining the f -values because $\tau_a \geq 2.5$.

1144 with $\pm 1 \sigma$ error estimates. We have allowed for a 4% zero-point uncertainty in the FUV lines. This seems prudent given that the observations were made through the LSA at wavelengths for which relatively little scattered-light information exists for the GHRS echelle modes.

Figure 3 shows the observed absorption profiles of several Fe II profiles from the μ Col data set with the component model overplotted. We have assumed the best-fit f -values derived through this method when displaying the λ 1143 and 1144 model profiles, namely $f = 0.0181$ and 0.120, respectively. The ticks above the λ 1143 and 1608 profiles show the locations of the centroids of the components in the assumed model (see Howk et al. 1999).

2.4. Curve-of-Growth Fitting Analysis

The ionic column densities along a sight line can be derived by fitting a curve of growth to the measured equivalent widths (Spitzer 1978; Jenkins 1986). Most often this approach assumes the absorption along a sight line can be approximated by a single Gaussian (Maxwellian) absorption model (e.g., Morton 1975). While this approximation is not always valid and can yield erroneous results, particularly when using lines of large peak optical depths (see, e.g., Jenkins 1987), it is possible to derive accurate column densities through this method (Jenkins 1986).

We use curve-of-growth fitting for the μ Col, ζ Oph, and δ Ori sight lines, using the equivalent widths given in Table 3, to derive oscillator strengths of the FUV Fe II f -values. To do this we fit a single-component Maxwellian curve of

growth to the NUV lines of Fe II for each star. Then, using the derived column densities and b -values, we determine the oscillator strength required to make the measured equivalent widths for each FUV line in Table 3 lie on the derived curve of growth. Recent studies have used similar curve-of-growth fitting techniques to derive oscillator strengths of C I (Zsargó, Federman, & Cardelli 1997), Ni II (Zsargó & Federman 1998), and Fe II (Cardelli & Savage 1995).

The results of this fitting process are summarized in Table 5. Figure 4 shows the curve of growth fitted to the measured equivalent widths for the μ Col sight line. The solid points show the NUV lines used to derive the curve of growth, while the open symbols show the FUV measurements assuming the final f -values summarized in Table 1. The derived sight line integrated column density, $\log N(\text{Fe II}) = 14.29 \pm 0.02$, is consistent with the value adopted by Howk et al. (1999), $\log N(\text{Fe II}) = 14.31 \pm 0.01$, based on component-fitting and apparent optical depth techniques. The best-fit b -value is $b = 12.9 \pm 0.2 \text{ km s}^{-1}$.

For the ζ Oph sight line we derive $\log N(\text{Fe II}) = 14.49 \pm 0.02$; Savage & Sembach (1996) derive $\log N(\text{Fe II}) = 14.51 \pm 0.02$. The best-fit b -value is $b = 6.6 \pm 0.2 \text{ km s}^{-1}$, consistent with the *Copernicus* study of Morton (1975). This curve of growth is shown in Figure 5. The FUV lines are placed on this diagram using the final f -values summarized in Table 1.

Toward δ Ori our best-fit curve of growth gives $\log N(\text{Fe II}) = 14.08 \pm 0.03$ and $b = 10.3 \pm 1.2 \text{ km s}^{-1}$; this fit is shown in Figure 6. We have not used the λ 2600 transition in constructing this fit given its very large optical depth (see

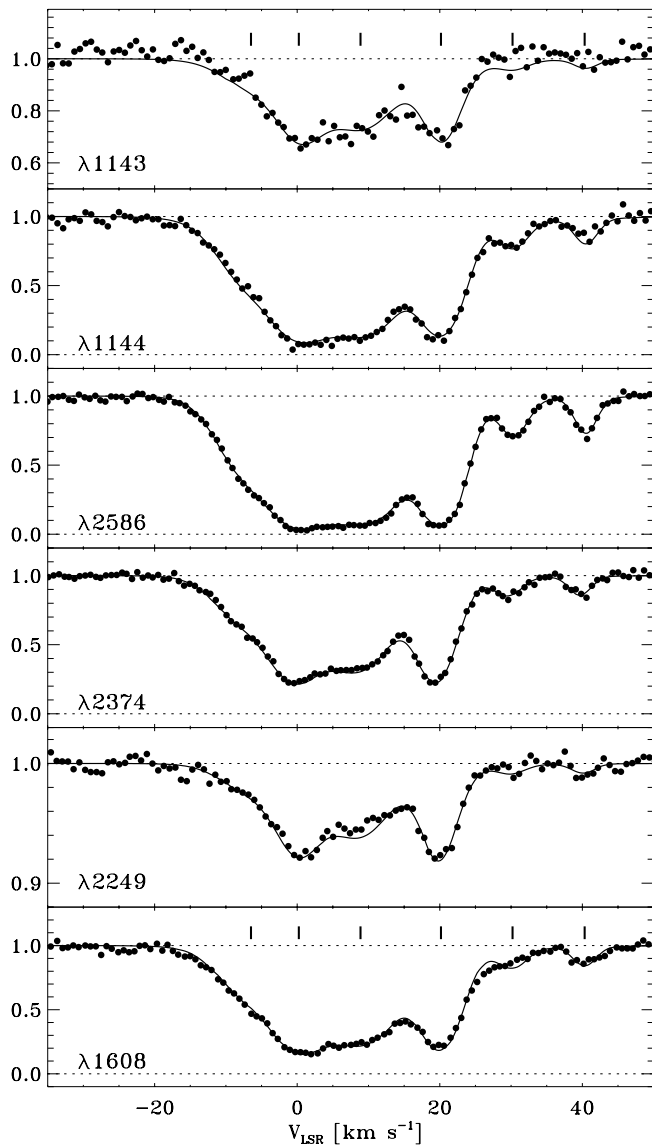


FIG. 3.—Continuum-normalized GHRS absorption-line spectra of several Fe II transitions toward μ Col. The filled dots show the GHRS data, while the solid lines show the best-fit component model of the absorption along this sight line. The ticks above the $\lambda\lambda 1608$ and 1143 profiles show the locations of the velocity centroids for the adopted component model. The model profiles use the f -values from Table 4, except for the $\lambda\lambda 1143$ and 1144 profiles. For these lines we use the best-fit f -values determined through our component-fitting analysis (see Table 1).

Jenkins 1987). For comparison, we derive $\log N_a(\text{Fe II}) = 14.08 \pm 0.02$ by a straight integration of the $N_a(v)$ profile of $\lambda 2260$. The peak apparent optical depth of this line is $\tau_a = 0.113 \pm 0.002$. An integration of the $\lambda 2374$ profile, which has a peak apparent optical depth of $\tau_a = 1.440 \pm 0.004$, yields $\log N_a(\text{Fe II}) = 14.02 \pm 0.01$. Although this suggests a modest degree of saturation in the $\lambda 2374$ profile (all in the component centered near $v_{\text{LSR}} \approx 10 \text{ km s}^{-1}$), this line is a factor of 15 stronger than the $\lambda 2260$ transition. Given the low optical depth of the $\lambda 2260$ absorption and the relatively weak saturation for the much stronger $\lambda 2374$ line, we believe the apparent column density derived from the $\lambda 2260$ profile is an accurate measure of the true column density, which is in agreement with that derived from our curve-of-growth fit.

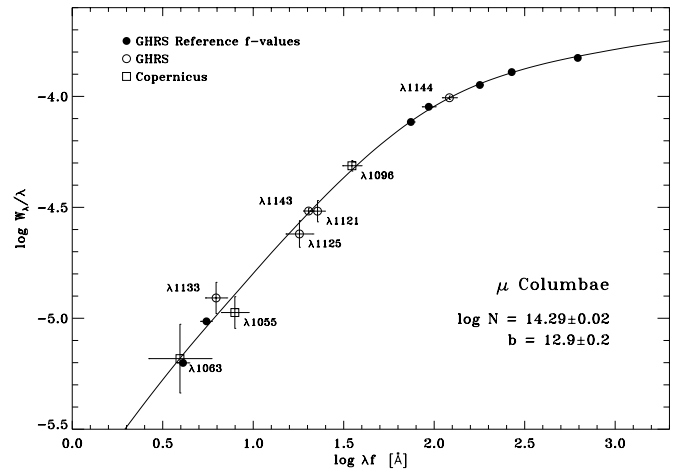


FIG. 4.—Best-fit, single-component curve of growth for the μ Col Fe II data. This curve was fitted to GHRS measurements of transitions with well-determined f -values (filled circles). The GHRS measurements (open circles) and Copernicus measurements (open squares) of FUV transitions are placed on this diagram using our final oscillator-strength estimates (see Table 1). The error bars in the equivalent-width measurements for the reference transitions are typically smaller than the filled plotting symbols. The column density derived from this curve of growth, $\log N(\text{Fe II}) = 14.29 \pm 0.02$, is consistent with the value $\log N(\text{Fe II}) = 14.31 \pm 0.01$, adopted by Howk et al. (1999) for this sight line using component-fitting techniques.

2.5. Summary of GHRS/Copernicus Oscillator-Strength Determinations

Table 5 summarizes the results of our f -value determinations using GHRS and Copernicus measurements. For each transition studied, this table gives the theoretically calculated f -value from RU98 and the unweighted mean, $\langle f_\lambda \rangle$, of our individual f -value determinations. Two measures of the errors in the mean are given: the formal statistical error and, where appropriate, the standard deviation of the individual measurements, f_λ^i , about the mean. Each of the individual f -value measurements are listed, along with the sight line, instrument, and method used to derive the individual measurement.

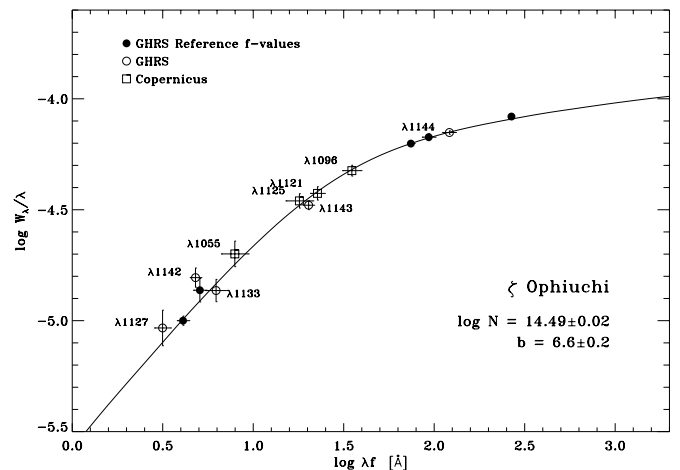


FIG. 5.—Same as Fig. 4, but for the sight line toward ζ Oph. The best-fit column density, $\log N(\text{Fe II}) = 14.49 \pm 0.02$, is consistent with the value $\log N(\text{Fe II}) = 14.51 \pm 0.02$ adopted by Savage & Sembach (1996).

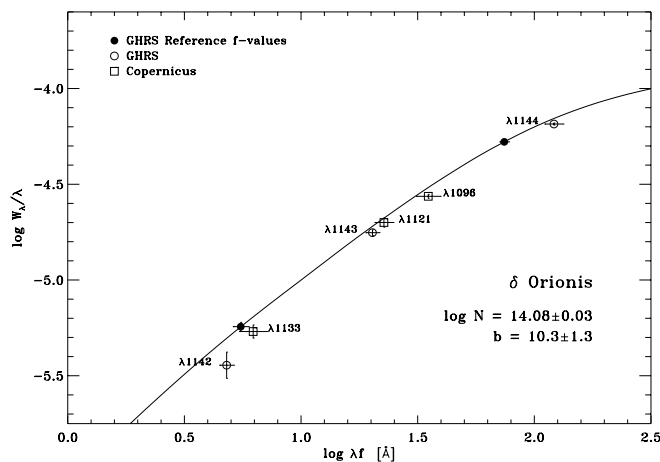


FIG. 6.—Same as Fig. 4, but for the sight line toward δ Ori. The best-fit column density is $\log N(\text{Fe II}) = 14.08 \pm 0.03$.

The oscillator strengths for the transitions at 1144.938, 1143.226, 1133.665, and 1125.448 Å all not only show good agreement with the theoretical values of RU98, but also have a reasonable number of consistent individual measurements. The determination of the $\lambda 1144$ oscillator strength could potentially be prone to systematic errors in the shape of the true curves of growth of the individual sight lines. As mentioned above, it is possible that the complicated, multi-component nature of the absorption along a given line of sight could cause the true curve of growth to deviate from the theoretical single-component Maxwellian curve used in our fits (see, e.g., Morton & Bhavsar 1979). Toward δ Ori, for example, $\lambda 1144$ is the strongest transition placed on the curve of growth and is thus somewhat sensitive to the adopted b -value, which is not terribly well constrained by

the weaker transitions. Toward μ Col and ζ Oph (to a somewhat lesser extent) this transition is well bracketed by secure measurements of the $\lambda 11608.451$ and 2586.650 lines. The agreement in the f -value derived for $\lambda 1144$ toward δ Ori with those derived for the other two sight lines is encouraging, suggesting that the systematics in the determination are within the range of the errors. It is also encouraging to note that the apparent optical depth, component-fitting, and curve-of-growth fitting results for μ Col are all in good agreement.

The $\lambda 1055.262$, 1063.972 , and 1142.366 transitions have formally calculated f -values that are consistent with the RU98 results. However, the individual measurements are sparse and often in poor agreement with one another. The oscillator strengths derived here for the $\lambda 1121.975$ and 1127.098 transitions are in poor agreement with the RU98 calculations, though there are a limited number of individual measurements for the latter line. In § 3 we use *FUSE* data to constrain the oscillator strengths of several of these lines.

3. FUSE MEASUREMENTS OF Fe II OSCILLATOR STRENGTHS AT FAR-ULTRAVIOLET WAVELENGTHS

We have derived oscillator strengths for several of the FUV Fe II transitions in the *FUSE* bandpass in § 2. The individual determinations of the f -values of Fe II $\lambda 1125.448$, 1133.665 , 1143.226 , and 1144.938 are in good agreement with one another. Furthermore, the oscillator strengths derived for these transitions are consistent with the theoretical calculations of RU98. We believe that the f -values for these FUV transitions, as given in Table 5, are secure, and we will use these oscillator strengths to derive estimates for the f -values of Fe II $\lambda 1112.048$, 1121.975 , 1127.098 , and 1142.366 using a suite of *FUSE* observations of absorption along extended path lengths through the Milky Way.

TABLE 6
FUSE OBSERVATION LOG

Star	Alternative Name	Data Set	Date ^a	Exposure Time (ks)	S/N ^b ($\lambda 1125$)	Notes
K1-16 ^c	I81103**	1999 Oct 15	40.0	30	CSPN
AV 232	Sk 80	X0200201	1999 Sept 25	10.3	18	SMC
HD 5980	Sk 78	X0240202	1999 Oct 20	3.2	18	SMC
Sk $-65^{\circ}22$	HD 270952	P1031002	1999 Dec 20	27.2	17	LMC
Sk $-67^{\circ}104$	HD 36402	P1031302	1999 Dec 17	5.1	13	LMC
Sk $-68^{\circ}80$	HD 36521	P1031402	1999 Dec 17	9.7	17	LMC
Sk $-69^{\circ}246$	HD 38282	P1031802	1999 Dec 16	22.1	10	LMC
Sk $-67^{\circ}211$	HD 269810	P1171603	1999 Dec 20	8.2	16	LMC
Sk $-67^{\circ}69$	P1171703	1999 Dec 20	6.2	8	LMC
Sk $-67^{\circ}167$	LH 76:21	P1171902	1999 Dec 17	2.8	11	LMC
Sk $-66^{\circ}100$	P1172303	1999 Dec 20	7.1	8	LMC
Sk $-70^{\circ}115$	HD 270145	P1172601	2000 Feb 12	5.2	13	LMC
BI 229	P1172801	2000 Feb 11	5.6	17	LMC
Sk $-67^{\circ}111$	LH 60:53	P1173001	2000 Feb 11	8.0	19	LMC
Sk $-69^{\circ}249$	HD 269927	P1174601	2000 Feb 9	7.2	23	LMC

^a Date of observation.

^b Empirical signal-to-noise ratio estimate near $\lambda 1125$ in the LiF1 channel.

^c The K1-16 data were obtained as part of in-orbit checkout activities. Since the object was observed at several different locations within the aperture, the processing of these data required special processing to ensure that the individual exposures were shifted and summed properly. This will be discussed in more detail by Kruk et al. 2000, in preparation.

The *FUSE* data used in this section, which are summarized in Table 6, were taken in late 1999/early 2000. Most of the stars in the current sample are located in the LMC, with two objects in the SMC and one in the Milky Way. We describe the details of the observations and reduction of the *FUSE* data sets in § 3.1. The use of these *FUSE* data to constrain the remaining Fe II oscillator strengths is described in § 3.2.

3.1. *FUSE* Observations and Data Reduction

The *FUSE* data for this investigation were obtained during the commissioning and early science operations stages of the *FUSE* mission. An observation log can be found in Table 6. Each observation was performed with the source centered in the $30'' \times 30''$ aperture of the LiF1 spectrograph channel.⁴ In many cases, the LiF2 channel was co-aligned well enough with the LiF1 channel that a second set of spectra covering the 1000–1187 Å wavelength range was obtained. Exposure times ranged from 3 to 27 ks

⁴ The K1-16 data were obtained as part of in-orbit checkout activities that required multiple exposures with the object at different locations within the aperture. The processing of this observation required special care to ensure that the individual exposures were shifted and summed properly. This will be discussed in more detail by Kruk et al. (2000, in preparation).

for the Magellanic Cloud stars observed. The time-tagged photon event lists were processed through the standard *FUSE* calibration pipeline (CALFUSE) available at the Johns Hopkins University. Pipeline Version 1.5.3 was used for the 1999 observations, and Version 1.6.8 was used for the 2000 February observations. The photon lists were screened for valid data with constraints imposed for Earth limb-angle avoidance and passage through the South Atlantic Anomaly. Corrections for detector backgrounds, Doppler shifts caused by spacecraft orbital motions, and geometrical distortions were applied (Sahnou et al. 2000; see also Blair et al. 2000).⁵ No corrections were made for optical astigmatism aberrations since the data were obtained prior to completion of in-orbit focusing activities. No flat-field solutions existed at the time of these observations; therefore, we compared the LiF1 and LiF2 spectra whenever possible to determine the significance of the observed features.

The processed data have a nominal spectral resolution of 20–25 km s^{−1} (FWHM), with a relative wavelength dispersion solution accuracy of ~ 6 km s^{−1} (1 σ). The zero point of the wavelength scale for each individual observation is poorly determined, although the absolute velocities of the

⁵ *FUSE* Observer's Guide, Version 2.0 (Blair et al. 2000) is available at <http://fuse.pha.jhu.edu/support/guide/guide.html>.

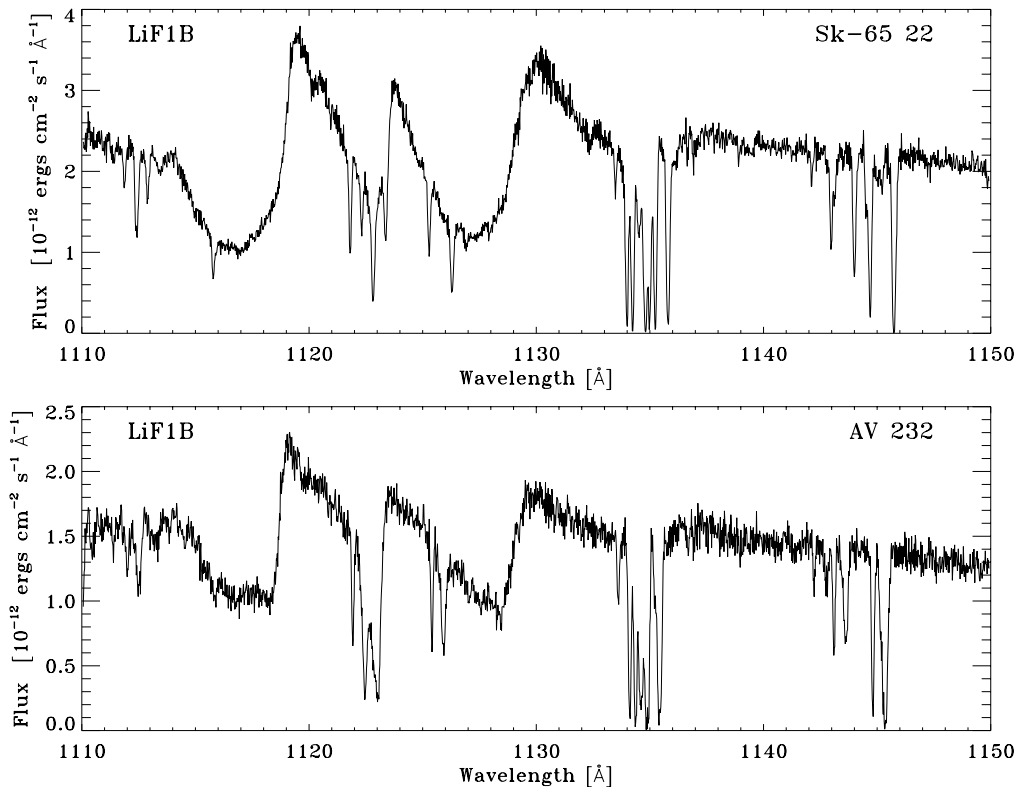


FIG. 7.—*FUSE* spectra of the O6 Iaf+ star Sk $-65^{\circ}22$ in the LMC (top) and the O7 Iaf+ star AV 232 in the SMC (bottom) over the range $1100 \lesssim \lambda \lesssim 1150$ Å. These plots show only data from the LiF1 channel, and the data have a resolution $\Delta v \gtrsim 20$ km s^{−1}. These spectra show absorption from interstellar Fe II in the Milky Way as well as both Magellanic Clouds at rest wavelengths of 1112.048, 1121.975, 1125.448, 1127.098, 1133.665, 1142.366, 1143.226, and 1144.938 Å. Also seen are interstellar lines of molecular hydrogen near 1112 Å, Fe III at 1122.524 Å, and a triplet of N I lines near 1135 Å. Several prominent P Cygni stellar-wind profiles are seen in this band, including the P v doublet at 1117.977 and 1128.008 Å and the Si IV lines at 1122.486 and 1128.339 Å.

material are not important for our purposes. When necessary, small velocity shifts were applied to individual spectral lines to ensure that the line-strength comparisons were judged over a common velocity scale. In particular, the lines at 1142, 1143, and 1144 Å were systematically shifted by -20 km s^{-1} with respect to those at 1112, 1121, and 1125 Å using the dispersion solution applied to the data used in this work.

Figure 7 shows portions of the *FUSE* spectra of two O-type stars: Sk $-65^\circ 22$ in the LMC and AV 232 in the SMC. These spectra represent only data from the LiF1 channel for each star. Most of the narrow interstellar lines in this bandpass are due to Fe II (see Table 1). Also present in these spectra are interstellar absorption from the Lyman (0-0) band of molecular hydrogen (near $\lambda\lambda 1110.1$, 1112.5, and 1115.5), from Fe III at 1122.5 Å and from a triplet of N I lines between 1134 and 1135 Å. These species are present in the Milky Way and the host galaxies of these stars, in some cases causing quite complex blending of the absorption. Prominent stellar-wind lines are also visible in this spectrum, particularly the strong P Cygni profiles of P v $\lambda\lambda 1118.0$ and 1128.0 and Si IV $\lambda\lambda 1122.5$ and 1128.3.

We have measured equivalent widths of the Fe II lines in the spectra of all of the stars listed in Table 6 in the same manner as described above for the GHRs data. The measured equivalent widths are summarized in Table 7. For gas arising in the LMC or SMC, many of the Fe II lines with well-determined f -values are blended or in regions of uncertain continuum placement. Hence, we only present the equivalent widths of absorption lines arising from gas in the Milky Way.

The values in Table 7 are averages of the equivalent widths measured in the LiF1B and LiF2A detector segments (where the latter were available). When comparing spectra taken through the LiF1 and LiF2 channels, there are occasionally differences in the profiles of absorption lines in the two channels. This seems to be associated with the greater degree of fixed-pattern noise in the LiF2A

channel. Typically these profile differences result in large discrepancies in the measured equivalent widths between the two channels. In cases where the LiF1 and LiF2 measurements differ by more than 2σ we have discarded the measurements from both channels.

3.2. Curve-of-Growth Fitting Analysis

Our determination of oscillator strengths using *FUSE* data relies on curve-of-growth fitting methods and follows the procedure discussed in § 2.4. We adopt the mean f -values of Fe II $\lambda\lambda 1125.448$, 1133.665, 1143.226, and 1144.938 from Table 1 as our reference oscillator strengths and use these to derive the f -values of $\lambda\lambda 1112.048$, 1121.975, 1127.098, and 1142.366. The results of this fitting procedure are summarized in Table 8. This table gives the individual f -value measurements, f_i^l , for each sight line. Given at the bottom of the table are the average, $\langle f_\lambda \rangle$, of our f -value determinations and the RU98 theoretical oscillator strengths for these transitions. The average $\lambda\lambda 1121$, 1127, and 1142 f -values were calculated using the *FUSE* determinations and the GHRs/*Copernicus* measurements given in Table 5. Also given with the average f -values are the statistical error (in parentheses) and standard deviation of the individual measurements about the mean (in brackets).

Two sample curves of growth are shown in Figure 8. These are toward the central star of a planetary nebula, K1-16, in the Milky Way and Sk $-65^\circ 22$ in the LMC. Each curve of growth represents only Galactic absorption. The best-fit column densities and b -values are shown on the plots. For the sight line toward Sk $-65^\circ 22$, the $\lambda 1143$ absorption is not available because of blending with LMC $\lambda 1142$ absorption.

Figure 9 shows the individual f -value determinations and error estimates for the $\lambda\lambda 1112.048$, 1121.975, 1127.098, and 1142.366 transitions. The ordinate of each panel shows the derived oscillator strength of the transition. Each measurement is offset along an otherwise meaningless abscissa. The open squares in Figure 9 mark measurements made using

TABLE 7
FUSE Fe II EQUIVALENT-WIDTH MEASUREMENTS

STAR	W_λ^a (mÅ)							
	$\lambda 1112.048$	$\lambda 1121.975$	$\lambda 1125.448$	$\lambda 1127.098$	$\lambda 1133.665$	$\lambda 1142.366$	$\lambda 1143.226$	$\lambda 1144.938$
K1-16	33 ± 2	92 ± 3	83 ± 3	18 ± 2	32 ± 3	28 ± 3	86 ± 3	171 ± 4
AV 232	45 ± 5	65 ± 6	63 ± 4	16 ± 4	42 ± 5	24 ± 4	76 ± 6	132 ± 4
HD 5980	64 ± 5	20 ± 4	34 ± 5	25 ± 6	60 ± 5	128 ± 4
Sk $-67^\circ 05^b$	85 ± 2	78 ± 2	16 ± 2	38 ± 5	16 ± 3	...	173 ± 4
Sk $-65^\circ 22$	28 ± 5	95 ± 5	70 ± 3	17 ± 4	29 ± 5	19 ± 3	...	192 ± 4
Sk $-67^\circ 104$	85 ± 6	73 ± 4	18 ± 5	37 ± 5	28 ± 5	...	148 ± 5
Sk $-68^\circ 80$	41 ± 4	84 ± 5	74 ± 3	16 ± 3	25 ± 4	21 ± 3	...	151 ± 4
Sk $-69^\circ 246$	42 ± 7	107 ± 6	87 ± 7	18 ± 4	25 ± 4	26 ± 3	...	213 ± 6
Sk $-67^\circ 211$	32 ± 4	104 ± 7	71 ± 5	16 ± 4	28 ± 5	39 ± 4	...	145 ± 10
Sk $-67^\circ 69$	40 ± 9	83 ± 8	80 ± 7	...	31 ± 4	18 ± 5	...	172 ± 9
Sk $-67^\circ 167$	74 ± 5	64 ± 5	...	27 ± 4	23 ± 4	69 ± 4	138 ± 4
Sk $-66^\circ 100$	40 ± 5	73 ± 5	72 ± 5	...	41 ± 6	23 ± 5	70 ± 6	125 ± 5
Sk $-70^\circ 115$	56 ± 6	96 ± 6	90 ± 5	...	31 ± 6	32 ± 5	93 ± 5	...
BI 229	19 ± 4	62 ± 3	55 ± 3	13 ± 4	27 ± 5	22 ± 3	76 ± 5	160 ± 6
Sk $-67^\circ 111$	29 ± 3	70 ± 4	64 ± 3	...	33 ± 3	22 ± 3	73 ± 3	145 ± 3
Sk $-69^\circ 249$	33 ± 4	91 ± 3	71 ± 3	14 ± 3	33 ± 3	29 ± 2

^a The equivalent-width measurements and 1σ errors given here are averages of the LiF1B and LiF2A observations for these sight lines.

^b The equivalent widths for Sk $-67^\circ 05$ are from Friedman et al. 2000.

TABLE 8
SUMMARY OF *FUSE* f -VALUE DETERMINATIONS

STAR	f_{λ}^i ^a			
	$\lambda 1112.048$	$\lambda 1121.975$	$\lambda 1127.098$	$\lambda 1142.366$
K1-16	0.0052(5)	0.0203(20)	0.0025(3)	0.0041(5)
AV 232	0.0082(15)	0.014(3)	0.0022(7)	0.0035(8)
HD 5980	0.0036(9)	0.0046(14)
Sk -67°05	0.0186(17)	0.0024(4)	0.0023(5)
Sk -65°22	0.0055(12)	0.025(3)	0.0031(9)	0.0035(7)
Sk -67°104	0.020(4)	0.0027(9)	0.0042(10)
Sk -68°80	0.008(4)	0.019(7)	0.0031(11)	0.0038(14)
Sk -69°246	0.0076(16)	...	0.0029(8)	0.0043(8)
Sk -67°211	0.0059(14)	0.035(12)	0.0026(9)	0.070(17)
Sk -67°69	0.0072(23)	0.019(4)	...	0.0028(9)
Sk -67°167	0.021(3)	...	0.0043(9)
Sk -66°100	0.0066(17)	0.017(4)	...	0.0032(10)
Sk -70°115	0.010(6)	0.019(11)	...	0.005(3)
BI 229	0.0043(10)	0.0167(21)	0.0027(10)	0.0046(8)
Sk -67°111	0.0055(8)	0.0175(22)	...	0.0039(6)
Sk -69°249	0.0076(16)	...	0.0029(8)	0.0043(8)
$\langle f_{\lambda} \rangle$ ^b	0.0062(9)[16]	0.0202(20)[46]	0.0028(3)[5]	0.0042(3)[11]
f_{RU98}	0.00446	0.0290	0.00112	0.00401

^a Individual measurements f_{λ}^i of the oscillator strengths with 1 σ errors in the last digit(s) given in parentheses.

^b Average value of f_{λ} with 1 σ statistical uncertainties of the last digits in parentheses. The standard deviations of the individual measurements f_{λ}^i about the mean are given in square brackets.

^c Theoretical values of f_{λ} from the calculations of Raassen & Uylings 1998.

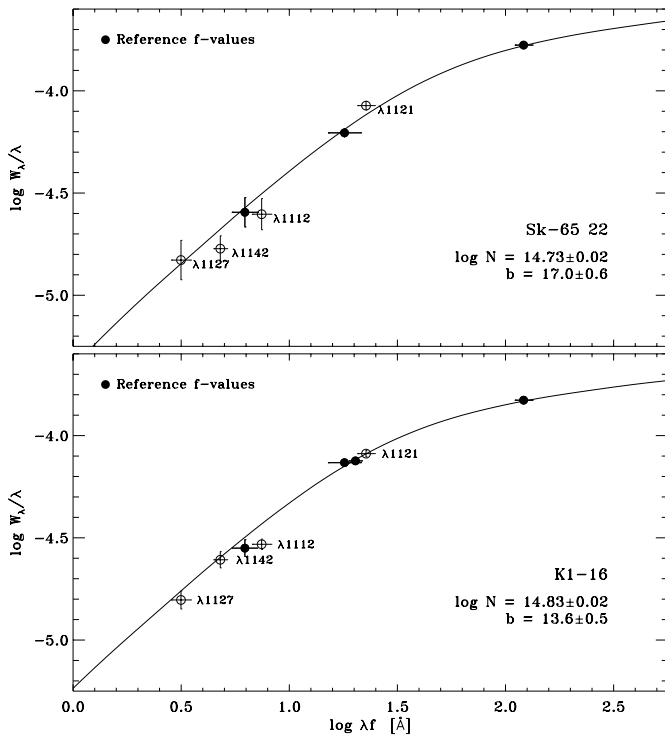


FIG. 8.—Best-fit, single-component curves of growth for the Sk -65°22 (top) and K1-16 (bottom) Fe II data. The curves were fitted to the $\lambda\lambda 1125$, 1133, 1143, and 1144 equivalent widths (filled circles), using RU98 the oscillator strengths. The open circles denote FUV transitions for which we have used the curves of growth to calculate the f -values. These transitions, at $\lambda\lambda 1112$, 1121, 1127, and 1142 are placed on the plots using our final oscillator-strength estimates (see Table 1). The column densities and b -values derived from these curves of growth are shown for each sight line. Toward Sk -65°22 these data sample only Milky Way material.

FUSE data (Table 8), while the filled circles mark estimates derived from GHRS and/or *Copernicus* data (Table 5). The dotted lines show the oscillator strengths calculated by RU98, while the thick-dashed lines show the unweighted means of the individual f -value determinations derived in this work.

Our measurements of the f -value for $\lambda 1142$ are consistent with the RU98 calculations. The empirically derived oscillator strengths of the remaining three lines, however, differ significantly from the theoretical values. Of these, the $\lambda 1121.975$ transition is the most prone to systematic uncertainties in the curve-of-growth fitting technique. Its strength places it between the $\lambda\lambda 1125$ and 1144 transitions. It is somewhat sensitive to the adopted b -value, which is determined in large part by the strong $\lambda 1144$ transition. This could, for sight lines whose curves of growth depart strongly from the single-component, Doppler-broadened model assumed here, potentially cause systematic uncertainties in our f -value determination. Furthermore, because we only measure one line stronger than the $\lambda 1121$ transition, the determination of b -values could be skewed by systematics in the measurement of the strong $\lambda 1144$ line. The good agreement of the three GHRS/*Copernicus* determinations of $f_{\lambda 1121}$, which are quite secure, with the majority of the *FUSE* determinations suggests that these systematics play a minor role. Systematics of this sort are likely of order $\lesssim 5\%$ given the agreement of the *FUSE* and GHRS/*Copernicus* determinations.

The systematic uncertainties are likely small for the weaker $\lambda\lambda 1112$, 1127, and 1142 transitions, which all fall on or near the linear part of the curve of growth for the sight lines studied. In these cases the systematics associated with measurements of weak interstellar lines in *FUSE* data are

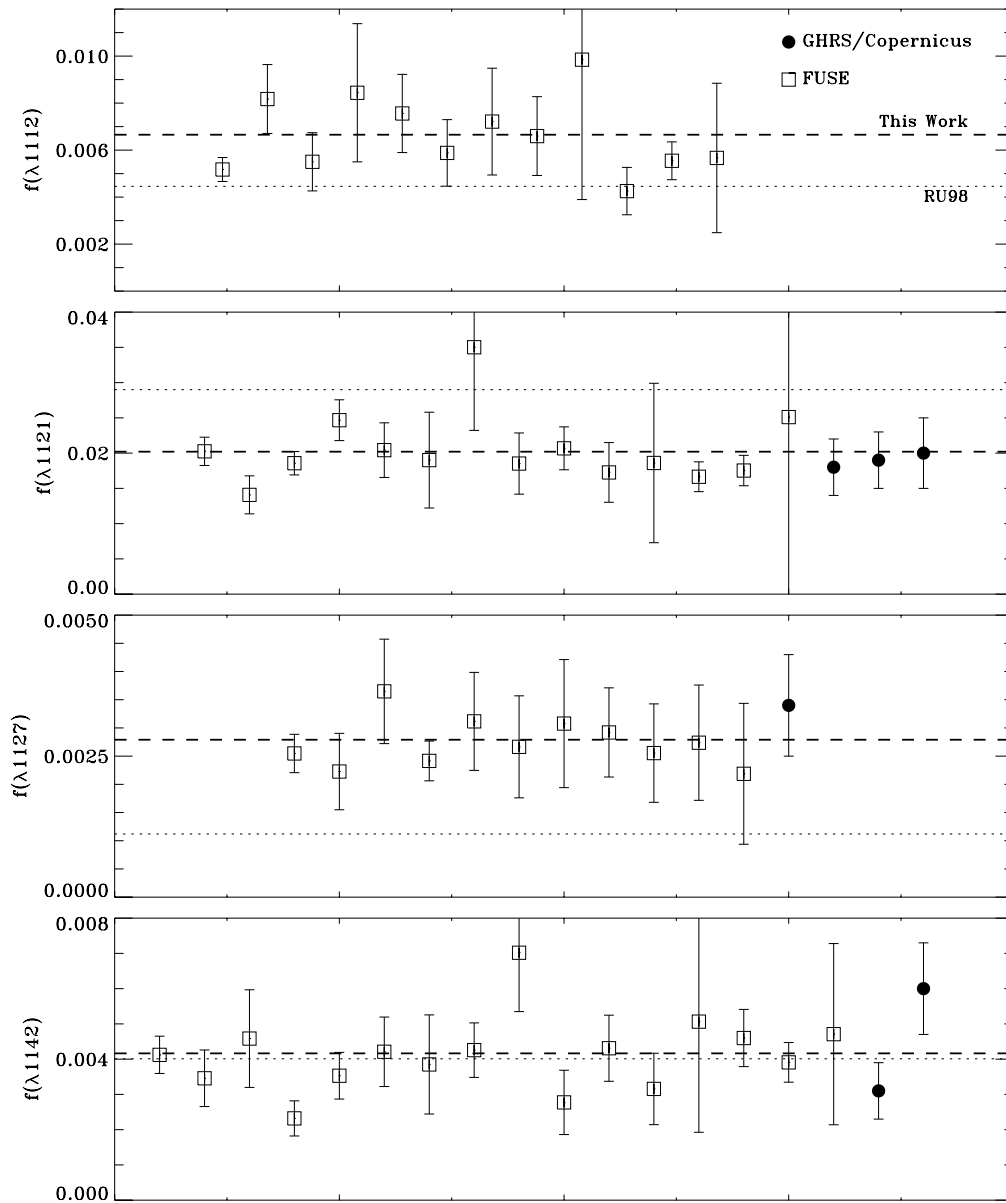


FIG. 9.—Distribution of the individual measurements f_{λ}^i of the oscillator strengths of $\lambda\lambda 1112.048$, 1121.975 , 1127.098 , and 1142.366 . The open squares represent estimates derived from *FUSE* data, while the filled circles denote estimates derived from GHRs and/or *Copernicus* data. The dotted lines show the oscillator strengths calculated by RU98, while the thick-dashed lines show the final average values derived in this work.

more important than the peculiarities of the fitting procedures. It should be noted that we have found no systematic differences across our sample of sight lines between the equivalent widths measured in the LiF1 and LiF2 channels for the weak $\lambda\lambda 1112$, 1127 , and 1142 transitions.

4. DISCUSSION AND SUMMARY

We have presented a self-consistent set of empirically derived f -values for the Fe II transitions in the range $1100 \lesssim \lambda \lesssim 1150$ Å, which are placed on an absolute scale by reference to the NUV laboratory measurements of Mullman et al. (1997) and Bergeson et al. (1994, 1996). The results of our work are summarized in Table 1, where we compare the empirically derived f -values from this work with previous theoretical and empirical determinations. Our derived oscil-

lator strengths agree with the orthogonal operator calculations of Raassen & Uylings (1998), with the exception of those at 1112.048 , 1121.975 , and 1127.098 Å. This is shown graphically in Figure 10, which displays the ratio of our best f -values to the theoretical f -values of RU98 versus their values. Over a factor of 30 range in oscillator strengths we find good agreement (within 1.5σ) between the RU98 strengths and those derived here for eight of the 11 lines studied in this work.

Our f -value determinations are in good agreement, for the most part, with the empirical results of Lugger et al. (1982) and Shull, van Steenberg, & Seab (1983). The empirical determinations by van Buren (1986) are at times in disagreement with our values. To some extent the agreement of our work with these empirical studies is expected since these

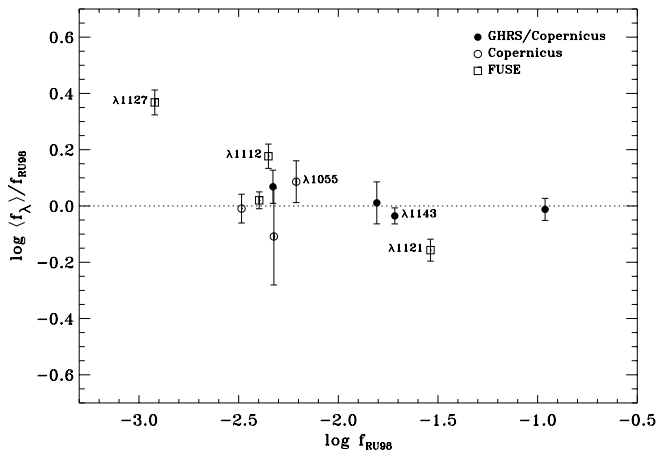


FIG. 10.—Ratio of the final average oscillator strengths derived in this work (see Table 1) to those calculated by RU98 vs. the RU98 strengths. Filled circles denote measurements that rely on *Copernicus* and/or GHRs data; the open circles are based only on *Copernicus* data; the open squares indicate estimates that include data from *FUSE*. In general, the agreement between our best empirically derived f -values and those calculated by RU98 is excellent. Important exceptions include the lines at 1112.048, 1121.975, and 1127.098 Å.

studies used curve-of-growth fitting methods (which carry the heaviest weight in our averages) for some of the same sight lines used here.

We note that our derived f -value for $\lambda 1142$, $f_{\lambda 1142} = 0.0042(3)$, is in disagreement with that of Cardelli & Savage

(1995), who derive $f_{\lambda 1142} = 0.00247(32)$ using GHRs observations of the star β^1 Scorpii. We believe our determination is more robust since it does not rely on a single measurement, although the dispersion of our measurements about the mean is relatively large for this transition. Welty et al. (1999b, their Appendix) discuss the potential discrepancies in FUV Fe II oscillator strengths, noting that the Cardelli & Savage (1995) f -value for $\lambda 1142$ might imply the need to revise the f -values of the $\lambda\lambda 1143$ and 1144 lines of the same multiplet. However, the RU98 calculations are in agreement with our empirical determinations for the FUV y^6F^o multiplet transitions out of the ground state.

As the *FUSE* mission proceeds there may be other opportunities (and requirements) for studying the atomic oscillator strengths at far-ultraviolet wavelengths. Some of the more important species for which it will be important to test the quality of the current oscillator strengths include O I, N I, and the shorter wavelength Fe II transitions. These species will be well observed by *FUSE* and will allow researchers to study the gas-phase abundances in a variety of environments, but only if the oscillator strengths are reasonably well known.

We thank E. Fitzpatrick for sharing his component-fitting software with us. This work is based on data obtained for the Guaranteed Time Team by the NASA-CNES-CSA *FUSE* mission operated by the Johns Hopkins University. Financial support to U.S. participants has been provided by NASA contract NAS 5-32985.

REFERENCES

- Bergeson, S. D., Mullman, K. L., & Lawler, J. E. 1994, *ApJ*, 435, L157
 Bergeson, S. D., Mullman, K. L., Wickliffe, M. E., Lawler, J. E., Litzén, U., & Johansson, S. 1996, *ApJ*, 464, 1044
 Blair, W. P., et al. 2000, *FUSE* Observer's Guide, Version 2.0
 Bohlin, R. C., Hill, J. K., Jenkins, E. B., Savage, B. D., Snow, T. P., Spitzer, L., & York, D. B. 1983, *ApJS*, 51, 277
 Cardelli, J. A., Ebbets, D. C., & Savage, B. D. 1990, *ApJ*, 365, 789
 ———, 1993, *ApJ*, 413, 401
 Cardelli, J. A., & Savage, B. D. 1995, *ApJ*, 452, 275
 Fitzpatrick, E. L. 1997, *ApJ*, 482, L199
 Fitzpatrick, E. L., & Spitzer, L. 1997, *ApJ*, 475, 623
 Friedman, S. D., et al. 2000, *ApJ*, 538, L39
 Howk, J. C., & Savage, B. D. 1999, *ApJ*, 517, 746
 Howk, J. C., Savage, B. D., & Fabian, D. 1999, *ApJ*, 525, 253
 Jenkins, E. B. 1986, *ApJ*, 304, 739
 ———, 1987, in *Interstellar Processes*, ed. D. J. Hollenbach & H. A. Thronson, Jr. (Dordrecht: Reidel), 533
 ———, 1996, *ApJ*, 471, 292
 Kurucz, R. L. 1988, *Trans. IAU*, 28, 168
 Lu, L., Sargent, W. L. W., Barlow, T. A., Churchill, C. W., & Vogt, S. 1996, *ApJS*, 107, 475
 Lu, L., Savage, B. D., Sembach, K. R., Wakker, B. P., Sargent, W. L. W., & Oosterloo, T. A. 1998, *AJ*, 115, 162
 Lugger, D., Barker, E., York, D. G., & Oegerle, W. 1982, *ApJ*, 259, 67
 Meyer, D. M., Cardelli, J. A., & Sofia, U. J. 1997, *ApJ*, 490, L103
 Meyer, D. M., Jura, M., & Cardelli, J. A. 1998, *ApJ*, 493, 222
 Moos, H. W., et al. 2000, *ApJ*, 538, L1
 Morton, D. C. 1975, *ApJ*, 197, 85
 Morton, D. C., & Bhavsar, S. P. 1979, *ApJ*, 228, 147
 Mullman, K. L., Sakai, M., & Lawler, J. E. 1997, *A&AS*, 122, 157
 Murphy, E. M., et al. 2000, *ApJ*, 538, L35
 Oegerle, W. R., et al. 2000, *ApJ*, 538, L23
 Pettini, M., Ellison, S. L., Steidel, C. C., & Bowen, D. V. 1999, *ApJ*, 510, 576
 Pettini, M., Smith, L. J., King, D. L., & Hunstead, R. W. 1997, *ApJ*, 486, 665
 Prochaska, J. X., & Wolfe, A. M. 1999, *ApJS*, 121, 369
 Raassen, A. J. J., & Uylings, P. H. M. 1998, *J. Phys. B*, 31, 3137 (RU98)
 Roth, K. C., & Blades, J. C. 1995, *ApJ*, 445, L95
 Sahnou, D. J., et al. 2000, *ApJ*, 538, L7
 Savage, B. D., Cardelli, J. A., & Sofia, U. J. 1992, *ApJ*, 401, 706
 Savage, B. D., & Sembach, K. R. 1991, *ApJ*, 379, 245
 ———, 1996, *ARA&A*, 34, 279
 Sembach, K. R., et al. 2000, *ApJ*, 538, L13
 Sembach, K. R., & Savage, B. D. 1992, *ApJS*, 83, 147
 ———, 1996, *ApJ*, 457, 211
 Shull, J. M., et al. 2000, *ApJ*, 538, L13
 Shull, J. M., van Steenberg, M., & Seab, C. G. 1983, *ApJ*, 271, 408
 Shull, J. M., & York, D. G. 1977, *ApJ*, 211, 803
 Sofia, U. J., Cardelli, J. A., & Savage, B. D. 1994, *ApJ*, 430, 650
 Sofia, U. J., Fabian, D., & Howk, J. C. 2000, *ApJ*, 531, 384
 Spitzer, L. 1978, *Physical Processes in the Interstellar Medium* (New York: Wiley)
 Spitzer, L., & Fitzpatrick, E. L. 1993, *ApJ*, 409, 299
 van Buren, D. 1986, *ApJ*, 311, 400
 Wakker, B. P., et al. 1999, *Nature*, 402, 388
 Welty, D. E., Frisch, P. C., Sonneborn, G., & York, D. G. 1999a, *ApJ*, 512, 636
 Welty, D. E., Hobbs, L. M., Lauroesch, J. T., Morton, D. C., Spitzer, L., & York, D. G. 1999b, *ApJS*, 124, 465
 Zsargó, J., & Federman, S. R. 1998, *ApJ*, 498, 256
 Zsargó, J., Federman, S. R., & Cardelli, J. A. 1997, *ApJ*, 484, 820